

THE GROWTH OF THE STELLAR SEEDS OF SUPERMASSIVE BLACK HOLES

JARRETT L. JOHNSON¹, DANIEL J. WHALEN², CHRIS L. FRYER³, AND HUI LI¹¹Nuclear and Particle Physics, Astrophysics and Cosmology Group (T-2), Los Alamos National Laboratory, Los Alamos, NM 87545²McWilliams Fellow, Department of Physics, Carnegie Mellon University, Pittsburgh, PA 15213³CCS-2, Los Alamos National Laboratory, Los Alamos, NM 87545

jlj@lanl.gov

Draft version March 2, 2018

ABSTRACT

The collapse of baryons into extremely massive stars with masses $\gtrsim 10^4 M_\odot$ in a small fraction of protogalaxies at $z \gtrsim 10$ is a promising candidate for the origin of supermassive black holes, some of which grow to a billion solar masses by $z \sim 7$. We determine the maximum masses such stars can attain by accreting primordial gas. We find that at relatively low accretion rates the strong ionizing radiation of these stars limits their masses to $M_* \sim 10^3 M_\odot (M_{\text{acc}}/10^{-3} M_\odot \text{ yr}^{-1})^{\frac{8}{7}}$, where M_{acc} is the rate at which the star gains mass. However, at the higher central infall rates usually found in numerical simulations of protogalactic collapse ($\gtrsim 0.1 M_\odot \text{ yr}^{-1}$), the lifetime of the star instead limits its final mass to $\sim 10^6 M_\odot$. Furthermore, for the spherical accretion rates at which the star can grow, its ionizing radiation is confined deep within the protogalaxy, so the evolution of the star is decoupled from that of its host galaxy. Ly α emission from the surrounding H II region is trapped in these heavy accretion flows and likely reprocessed into strong Balmer series emission, which may be observable by the *James Webb Space Telescope*. This, along with strong He II λ 1640 and continuum emission, are likely to be the key observational signatures of the progenitors of supermassive black holes at high redshift.

Subject headings: stars: formation - accretion - ISM: H II regions - cosmology: early universe - theory - galaxies: formation

1. INTRODUCTION

The existence of $10^8 - 10^9 M_\odot$ black holes (BH) in massive galaxies by $z \sim 7$, less than a billion years after the Big Bang (Fan et al. 2003; Willott et al. 2003; Mortlock et al. 2011), remains one of the great mysteries of cosmological structure formation. In the Λ CDM paradigm, early structure formation is hierarchical, with small dark matter halos at early epochs evolving into ever more massive ones by accretion and mergers through cosmic time. Hence, it is generally held that the supermassive black holes (SMBH) of the $z \sim 7$ *Sloan Digital Sky Survey* (SDSS) quasars grow from much smaller seeds at high redshifts. The origin of these seeds, and how they reach such large masses by such early times, remains to be understood. At least four main processes have been proposed for their formation (see Volonteri 2010; Alexander & Hickox 2011; Khlopov 2010): the collapse of Pop III stars into 100 - 300 M_\odot BH at $z \sim 20$ (e.g. Madau & Rees 2001; Alvarez et al. 2009; Milosavljević et al. 2009; Tanaka & Haiman 2009), the direct collapse of extremely hydrogen molecule-poor primordial gas in $\sim 10^8 M_\odot$ dark matter halos into $10^4 - 10^6 M_\odot$ BH at $z \sim 10$ (e.g. Bromm & Loeb 2003; Koushiappas et al. 2004; Begelman et al. 2006; Lodato & Natarajan 2006; Spaans & Silk 2006; Omukai et al. 2008; Regan & Haehnelt 2009; Sethi et al. 2010; Inayoshi & Omukai 2011, see also Colgate et al. 2003), the collapse of dense primeval star clusters into $10^4 - 10^6 M_\odot$ BH (see e.g. Djorgovski et al. 2008; Devecchi & Volonteri 2009), and the collapse of primordial overdensities in the immediate aftermath of the Big Bang (see e.g. Mack et al. 2007; Carr et al. 2010).

The processes by which black holes form at high red-

shift and evolve into SMBH must account for how they become so large by $z \sim 7$ and why their numbers at that redshift are so small, about 1 Gpc^{-3} . Pop III seed BH are plentiful at $z \sim 20 - 30$ but must grow at the Edington limit without interruption to reach $10^8 - 10^9 M_\odot$ by $z \sim 7$. This is problematic because they and their progenitors either expel all the baryons from the shallow potential wells of the halos that create them, so they are "born starving" (Whalen et al. 2004; Johnson & Bromm 2007; Pelupessy et al. 2007; Alvarez et al. 2009; Jeon et al. 2011), or they eject themselves from their halos, and thus their fuel supply, at hundreds of km/s if they are born in core-collapse supernova explosions (Whalen & Fryer 2011 in prep). Also, accretion onto Pop III BH has been found to be inefficient on small scales, typically at most 20% Edington (Milosavljević et al. 2009; Park & Ricotti 2011), making the constant duty cycles required for sustained growth difficult (but see Li 2011).

If halos can instead congregate into primitive galaxies of $\sim 10^8 M_\odot$ at $z \sim 10 - 15$ that are devoid of the coolant molecular hydrogen (H_2), they reach virial temperatures of $\sim 10^4 \text{ K}$ and begin to atomically cool. Numerical simulations of this process (Wise et al. 2008; Regan & Haehnelt 2009; Shang et al. 2010) find that in analogy to Pop III star formation in much smaller halos at higher redshifts (Nakamura & Umemura 2001; Bromm et al. 2002; Abel et al. 2002; O'Shea & Norman 2007; Yoshida et al. 2008; Turk et al. 2009; Stacy et al. 2010; Clark et al. 2011; Greif et al. 2011), baryons rapidly pool at the center of the halo and form a hydrostatic object. But this object is thought to become far more massive than Pop III stars modeled to date because atomic line cooling and the deeper potential well of the halo lead to much

higher infall rates at its center, $0.1 - 1 M_{\odot} \text{ yr}^{-1}$ rather than the $10^{-4} M_{\odot} \text{ yr}^{-1}$ typical of primordial star-forming minihalos at $z \sim 20$. Such objects could collapse into black holes that are far more massive than Pop III BH (e.g. Shibata & Shapiro 2002), with Bondi-Hoyle accretion rates that allow them to grow into SMBH in less time (e.g. Wyithe & Loeb 2011; but see Dotan et al. 2011).

One difficulty with this scenario is that it is not yet understood how primitive galaxies can form in the high Lyman-Werner UV backgrounds needed to fully suppress H_2 molecule formation and quench Pop III star formation in its constituent halos prior to assembly (1 - 10 times those expected at the epoch of reionization at $z \sim 6$; Dijkstra et al. 2008; Shang et al. 2010; Wolcott-Green et al. 2011, see also Agarwal et al. in prep). Furthermore, it is not known if the object at the center of the protogalaxy even becomes a star, because at such high accretion rates it reaches very large masses on timescales that are short in comparison to Kelvin-Helmholtz times and the onset of nuclear burning (although Ohkubo et al. 2009 have modeled the evolution of Pop III stars under accretion at much lower rates). It could be that the central object reaches such high entropies and densities that it is enveloped by an event horizon before reaching the main sequence (Fryer et al. 2001). If the central object becomes a star, what governs its rate of growth, its final mass, and thus the mass of the SMBH seed it becomes? Numerous authors have studied how stellar radiation regulates accretion onto Pop III protostars, but at much lower inflow rates than those in the centers of collapsing protogalaxies (e.g. Stahler et al. 1986; Omukai & Palla 2001; Omukai & Inutsuka 2002; McKee & Tan 2008; Stacy et al. 2011a; Hosokawa et al. 2011). Do the much higher accretion rates in primitive galaxies quench radiative feedback?

We have performed extensive semianalytical calculations of radiative feedback by Pop III supermassive stars in collapsing protogalaxies at $z \sim 10$. In §2, we examine the primary forms of radiative feedback on accretion onto the star (deferring the processes that can be ignored to thorough examination in the Appendix). We also derive the maximum mass that the supermassive star, and hence the SMBH seed, can achieve as a function of accretion rate, accounting for its prodigious ionizing UV flux. In §3, we estimate the maximum mass that the star can reach if it is limited by its finite lifetime rather than by radiative feedback. We discuss the observational signatures of rapidly accreting supermassive primordial stars in §4. Finally, in §5 we review the implications of final supermassive stellar mass for SMBH seed mass and the appearance of the first quasars in the Universe.

2. RADIATIVE FEEDBACK-LIMITED ACCRETION

We adopt an analytical approach to estimate the maximum mass that an accreting primordial star can ultimately attain in a collapsing $10^7 - 10^8 M_{\odot}$ protogalaxy. For simplicity, we assume that accretion onto the star is constant and spherically-symmetric. We first consider the ionizing UV radiation emitted by the star, which is the dominant form of radiative feedback on the infall and envelops the star with an H II region. In particular, we make the following assumptions on the nature of the radiative feedback on the accretion flow (see Fig. 1):

(1) Outside the H II region, gas is accelerated only by gravity and falls inwards unchecked by gas or radiation pressure.

(2) Within the H II region, the gas is decelerated due to photoionization pressure only. This follows from the fact that the massive stars we consider here radiate at very nearly the Eddington limit. By definition, this implies that the force due to electron scattering in the H II region exactly cancels that due to gravity; therefore, for simplicity we can assume that the only net force on the gas is due to photoionization pressure (see also Omukai & Inutsuka 2002).

In this Section we first determine how ionizing radiation from the supermassive star limits its growth via accretion. We then consider the effect of the $\text{Ly}\alpha$ photons to which the majority of the energy in the ionizing radiation is converted. We examine and exclude other processes that can contribute to feedback on accretion in the Appendix.

2.1. Suppression of Accretion by Photoionization

As we are considering constant, spherically-symmetric accretion, the equation that links the number density n of hydrogen nuclei and the velocity v of the gas at a distance r from the star is:

$$n(r) = \frac{\dot{M}_{\text{acc}}}{4\pi r^2 v(r) \mu m_{\text{H}}} . \quad (1)$$

Here, we assume that the gas is primordial with an average atomic weight of $\mu m_{\text{H}} = 1.2 m_{\text{H}}$, where m_{H} is the mass of the hydrogen atom.

Because the ionizing photons are trapped within the H II region, we assume that the velocity of the gas at its edge, at a distance r_{HII} , is just the free-fall velocity:

$$v(r_{\text{HII}}) = - \left(\frac{2GM_*}{r_{\text{HII}}} \right)^{\frac{1}{2}} . \quad (2)$$

We note that this velocity is much higher than the sound speed of the gas, at which infall is found to proceed from large radii in cosmological simulations (Wise et al. 2008; Shang et al. 2010; Johnson et al. 2011), so we neglect this small contribution to the gas velocity for simplicity.

The radius of the H II region, r_{HII} , is determined by the ionization front jump conditions, which require a balance between the rate Q at which ionizing photons are emitted from the star and the sum of the rate of hydrogen recombinations in the ionized volume (first term on the RHS in equation 3) and the rate at which neutral atoms enter the H II region through the accretion flow (second term on the RHS in equation 3). Following Raiter et al. (2010), we note that the rate at which ionizations occur is higher than Q by a factor P which accounts for corrections to the neutral hydrogen level populations at the high temperatures ($\simeq 2-4 \times 10^4 \text{ K}$; e.g. Whalen et al. 2004; Alvarez et al. 2006) expected for the H II regions of massive Pop III stars. To account for this rate, we take it that the total ionization rate in the H II region is $Q_{\text{eff}} = PQ$, where P is the ratio of the average ionizing photon energy and the ionization potential for neutral hydrogen, 13.6 eV. Integrating over the density profile of the gas in eq. 1 to find the radius at which the total number of recombinations in the enclosed volume balances the total number of

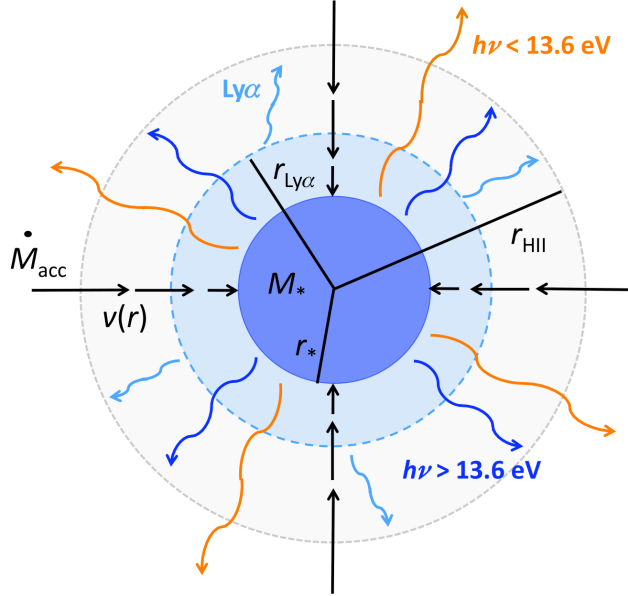


FIG. 1.— Schematic representation of accretion onto a supermassive Pop III star of mass M_* and radius r_* . Gas accretes at a constant rate \dot{M}_{acc} , being acted upon only by gravity at $r > r_{\text{HII}}$, the radius of the H II region of the star. Inside r_{HII} the gas, whose infall velocity is $v(r)$, is decelerated by momentum absorbed during ionizations, which is indicated by the shortening of the velocity vector arrows. While continuum photons with energies $h\nu < 13.6$ eV escape the H II region and do not couple strongly to the gas even outside r_{HII} , resonant line photons do couple strongly and so in principle can also impart momentum to the gas. In particular, a large amount of momentum is emitted by H I recombinations as Ly α ; however, these photons couple so strongly to the gas that within $r_{\text{Ly}\alpha}$ more than 50 percent of the emission is trapped in the accretion flow and cannot propagate outward and affect the dynamics of the flow. Within r_{HII} , Ly α photons are reprocessed into Balmer series photons which escape the H II region and may provide an observable signature of accreting supermassive stars (see §4).

photoionizations, we arrive at the following expression for r_{HII} :

$$Q_{\text{eff}} \simeq \int_{r_*}^{r_{\text{HII}}} 4\pi\alpha_{\text{B}}r^2n^2dr + \frac{\dot{M}_{\text{acc}}}{\mu m_{\text{H}}} \\ = \int_{r_*}^{r_{\text{HII}}} 4\pi\alpha_{\text{B}}r^2 \left[\frac{\dot{M}_{\text{acc}}}{4\pi r^2 v(r) \mu m_{\text{H}}} \right]^2 dr + \frac{\dot{M}_{\text{acc}}}{\mu m_{\text{H}}}, \quad (3)$$

where $\alpha_{\text{B}} \simeq 1.4 \times 10^{-13} \text{ cm}^3 \text{ s}^{-1}$ is the recombination coefficient for $\gtrsim 2 \times 10^4$ K photoionized primordial gas (Whalen et al. 2004; Osterbrock & Ferland 2006). Following Omukai & Inutsuka (2002), for simplicity we neglect the second term in our calculations, as it is in general much smaller than Q_{eff} . This is true in particular for the solutions that we find for the minimum accretion rate onto a star of a given mass; at much higher rates, this term may become large, likely limiting the radius of the H II region.

Finally, once the accreting gas crosses the stationary ionization front (as shown in Fig. 1), the equation that governs its deceleration due to momentum imparted by photoionizations is:

$$v \frac{dv}{dr} = -\frac{\alpha_{\text{B}} h \nu n}{\mu m_{\text{H}} c} = -\frac{\alpha_{\text{B}} h \nu}{\mu m_{\text{H}} c} \left[\frac{\dot{M}_{\text{acc}}}{4\pi r^2 v(r) \mu m_{\text{H}}} \right], \quad (4)$$

where again we have assumed that the photoionization rate of hydrogen is balanced its recombination rate, $\alpha_{\text{B}} n$, and that the momentum transferred to the gas per photoionization is $h\nu/c$. We note again that here we have not

included the force due to gravity or that due to Thomson scattering, as these two forces cancel one another since the star is assumed to radiate at the Eddington rate. For the massive primordial stars that we consider here, we take the effective surface temperature of the star to always be $\simeq 10^5$ K, which yields an average energy per ionizing photon $h\nu \simeq 29$ eV. In turn, this implies $P \equiv h\nu/13.6 \text{ eV} = 2.1$, which we assume throughout our study. In equation (4) we again choose case B, as we assume that recombinations to the ground level of hydrogen result in the emission of photons which do not deposit a net momentum to the gas (being emitted isotropically and contributing to the diffuse radiation field).¹

To find the solutions for steady state accretion, we must solve the equation of motion equation 4. In particular, to find the minimum accretion rate for which an inflow solution exists, we search for solutions for which the infall velocity of the gas goes to zero at the stellar surface r_* :

$$v(r_*) = 0. \quad (5)$$

That is, we must simultaneously solve equations 3 and 4, under the constraints given by equations 2 and 5. These constraints yield the maximum mass that the star can achieve by steady accretion before its intense ionizing radiation halts infall at $r > r_*$ and prevents its further growth. On the other hand, they also yield the lower bound for the final mass of the central object, since for $v(r_*) > 0$ radiative feedback fails to cut off accretion and the star will grow even faster than when gas merely comes to a halt on

¹ At the high densities in the H II regions we consider (Fig. 2) and with the enhanced population of neutral hydrogen in the $n = 2$ state due high temperatures in primordial H II regions (Raiter et al. 2010), a ~ 30 percent smaller 'extended case B' (Hummer & Storey 1987) recombination coefficient may be more appropriate, but our final results are not strongly dependent on this choice.

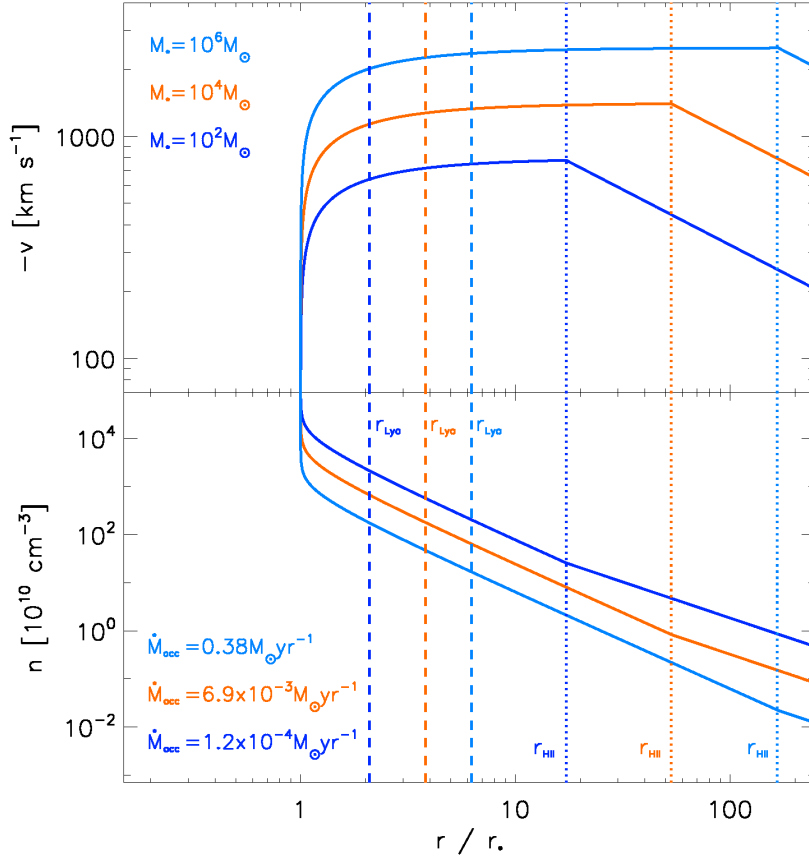


FIG. 2.— The infall velocity (*top panel*) and density (*bottom panel*) of the gas accreting onto primordial stars as a function of distance r from the center of the star for three stellar masses: 10^2 (dark blue), 10^4 (red), and $10^6 M_\odot$ (light blue). Each star accretes at the minimum rate (as labeled) its strong ionizing flux permits, as given by equation 11. The dotted lines show the radius r_{HII} of the H II regions surrounding the stars, with their colors corresponding to those of the respective stellar masses. Outside the H II region, the gas is in free-fall, but after crossing into the H II region boundary it is rapidly photoionized and decelerated until it arrives at the stellar surface with velocity $v(r_*) = 0$. The dashed lines show the trapping radius $r_{\text{Ly}\alpha}$ for Ly α photons from recombinations in the H II region (assuming a gas temperature of 4×10^4 K, see equation 22); partly because the vast majority of these photons are trapped within $r_{\text{Ly}\alpha}$, we can neglect Ly α scattering feedback as discussed in §2.2. Accretion at rates below those shown here is not possible, as in such cases $r_{\text{HII}} \rightarrow \infty$ and photoionization pressure halts infall at all radii.

its surface.

The solution to equation 4 has the general form

$$v(r) = \left[\left(\frac{3\alpha_B h\nu \dot{M}_{\text{acc}}}{4\pi\mu^2 m_{\text{H}}^2 c} \right) r^{-1} - K \right]^{\frac{1}{3}}, \quad (6)$$

where K is a constant whose value must satisfy the constraint that $v(r_*) = 0$. This yields for K

$$K = \left(\frac{3\alpha_B h\nu \dot{M}_{\text{acc}}}{4\pi\mu^2 m_{\text{H}}^2 c} \right) r_*^{-1}. \quad (7)$$

The equation for the infall velocity in the H II region then becomes

$$v(r) = \left[\left(\frac{3\alpha_B h\nu \dot{M}_{\text{acc}}}{4\pi\mu^2 m_{\text{H}}^2 c} \right) r^{-1} - \left(\frac{3\alpha_B h\nu \dot{M}_{\text{acc}}}{4\pi\mu^2 m_{\text{H}}^2 c} \right) r_*^{-1} \right]^{\frac{1}{3}}. \quad (8)$$

As shown in Figure 2, these solutions give a relatively constant velocity for the gas in the H II region until it is very

close to the stellar surface. In turn, equation (1) implies that $n(r)$ is essentially $\propto r^{-2}$ in the H II region.

Applying this $v(r)$ (and hence $n(r)$) to the integral in equation 3 and evaluating it yields r_{HII} :

$$r_{\text{HII}} = \left[r_*^{-1} - \frac{4\pi Q_{\text{eff}}^3}{3\alpha_B} \left(\frac{h\nu\mu m_{\text{H}}}{c} \right)^2 \dot{M}_{\text{acc}}^{-4} \right]^{-1}. \quad (9)$$

Finally, we must satisfy the constraint given by equation 2 to find the solution for the minimum accretion rate. Substituting equations 8 and 9 into equation 2 and rearranging the terms gives the following quadratic equation in \dot{M}_{acc}^2 :

$$0 = \left(\frac{2GM_*}{r_*} \right) \dot{M}_{\text{acc}}^4 - \left(\frac{Q_{\text{eff}} h\nu}{c} \right)^2 \dot{M}_{\text{acc}}^2 - \frac{8\pi GM_* Q_{\text{eff}}^3}{3\alpha_B} \left(\frac{h\nu\mu m_{\text{H}}}{c} \right)^2, \quad (10)$$

whose solution is

$$\dot{M}_{\text{acc}}^2 = \frac{\left(\frac{Q_{\text{eff}} h\nu}{c}\right)^2 + \left[\left(\frac{Q_{\text{eff}} h\nu}{c}\right)^4 + \frac{64\pi Q_{\text{eff}}^3}{3\alpha_{\text{B}} r_*} \left(\frac{GM_* h\nu \mu m_{\text{H}}}{c}\right)^2\right]^{\frac{1}{2}}}{\frac{4GM_*}{r_*}}. \quad (11)$$

Noting that the second term in the square brackets is much larger than the first, we have

$$\dot{M}_{\text{acc}} \simeq \left(\frac{4\pi Q_{\text{eff}}^3 r_*}{3\alpha_{\text{B}}} \left(\frac{h\nu \mu m_{\text{H}}}{c}\right)^2\right)^{\frac{1}{4}}, \quad (12)$$

which exactly matches the accretion rate for which the H II region breaks out to infinity (see equation 9) and therefore stops accretion entirely because photoionization pressure exerts a net outward force on gas at all radii.² Thus, we see that the H II region is confined and that accretion proceeds at infall rates higher than those given by equation 12 and that no inflow solutions exist for lower rates.³

Now, by expressing Q (where again $Q_{\text{eff}} = PQ$, with $P = 2.1$) and r_* just in terms of the stellar mass M_* , we can find the maximum stellar mass for which accretion onto the star is permitted (at \dot{M}_{acc} in equation 12). We can take it that, if the star is thermally relaxed⁴ and radiating at the Eddington limit (Begelman 2010), then the following two equations relate the mass M_* of the star to its ionizing photon emission rate Q and radius r_* :

$$Q = 1.6 \times 10^{50} \text{ s}^{-1} \left(\frac{M_*}{100 M_{\odot}}\right), \quad (13)$$

and

$$r_* = 3.7 R_{\odot} \left(\frac{M_*}{100 M_{\odot}}\right)^{\frac{1}{2}}. \quad (14)$$

These are from Table 1 of Bromm et al. (2001) and are in good agreement with Schaerer (2002) and Begelman (2010). With these expressions, we find that the solution to equation 12 is

$$M_* \simeq 10^3 M_{\odot} \left(\frac{\dot{M}_{\text{acc}}}{10^{-3} M_{\odot} \text{ yr}^{-1}}\right)^{\frac{8}{7}}, \quad (15)$$

where M_* is the maximum stellar mass attainable under accretion of gas at a rate \dot{M}_{acc} .

We plot this maximum stellar mass in Figure 3. As we shall see, the feedback due to ionizing radiation emitted by the star can limit its mass at relatively low accretion rates, which we term 'feedback-limited accretion'. However, at higher accretion rates the finite lifetime of the star governs its maximum mass; we term this 'time-limited accretion'. We discuss why this is so in § 3.

Although we have focused on the pressure due to hydrogen photoionizations, it is straightforward to include

² While in our solution the H II region formally extends to infinity in this case, for accretion to be terminated it need only extend to the Bondi radius, outside of which gas cannot be gravitationally captured by the star.

³ Relatively small deviations from the solutions we have found for $v(r)$ at r_{HII} may result in a shock developing there. However, even for a strong shock for which there is a density jump of a factor of four, the minimum accretion rates in equation 11 change by $\lesssim 20$ percent.

⁴ At the minimum accretion rates we find for a given stellar mass (equation 15), the 'trapping' radius due to electron scattering (which is proportional to the accretion rate, e.g. Begelman 1978) is always smaller than the stellar radius given by equation 14. Therefore, the main sequence stars we consider here are thermally relaxed (see also Ohkubo et al. 2009). At higher accretion rates, the radiation emitted by the star can become trapped due to electron scattering, resulting in an expansion of the stellar photosphere. In this case the star emits fewer ionizing photons than given by equation (13) and the radiative feedback is thus weakened, as we discuss briefly in the appendix.

⁵ We note that in the high densities in the H II regions we consider (see Fig. 2), frequent collisions can prevent the radiative decay of hydrogen via two photon emission, which raises the Ly α luminosity above that expected in the low density regime, where $\beta_{\text{Ly}\alpha} \simeq 0.68$ (Spitzer 1978).

He I photoionizations under the condition that within the H II region He I is also photoionized to He II. For the relatively hard spectra of massive primordial stars this is a sound assumption because the number of He I-ionizing photons is comparable to the number of H I-ionizing photons (Schaerer 2002). The ratio of the radiation pressures from helium and hydrogen photoionization is then

$$\frac{p_{\text{HeI}}}{p_{\text{HI}}} \simeq \frac{n_{\text{He}} h\nu_{\text{HeI}} \alpha_{\text{B,HeI}}}{n_{\text{H}} h\nu_{\text{HI}} \alpha_{\text{B,HI}}} \simeq 0.14, \quad (16)$$

where the first term is the ratio of helium and hydrogen number densities, which is $\simeq 0.1$. The second term is the ratio of the average ionizing photon energies for He I and H I, which by integrating the stellar spectrum of a 10^5 K primordial star we find to be $38 \text{ eV}/29 \text{ eV} \simeq 1.3$. The third term is the ratio of He I and H I case B recombination coefficients, which is $\simeq 1.1$ (Osterbrock & Ferland 2006). While this is a relatively modest increase in the radiation pressure, for completeness we include it as a multiplicative coefficient when solving equation 4. Other forms of radiation pressure are not so easily accommodated by our analytical approach but can be neglected without strongly affecting our conclusions, as we discuss in the next Section and in the Appendix.

2.2. Trapping of Ly α photons

In the H II region of the accreting star, a large fraction of the ionizing radiation is reprocessed into Lyman α photons, which couple very strongly to primordial gas and could impart significant momentum to it, as they in principle can scatter many times across the H II region (e.g. Doroshkevich & Kolesnik 1976; Oh & Haiman 2002; McKee & Tan 2008). However, while these authors showed that scattering Ly α can strongly counteract the accretion flow at relatively low accretion rates, at the extremely high rates under which supermassive stars grow (e.g. $\dot{M}_{\text{acc}} \gtrsim 10^{-2} M_{\odot} \text{ yr}^{-1}$) the impact on the accretion flow is reduced due both to the large momentum of the infalling gas and to the trapping of Ly α photons within the H II region.

To show this, we first compare the momentum in Ly α photons to the momentum of the accretion flow. The former is given by (Raiter et al. 2010)

$$\frac{L_{\text{Ly}\alpha}}{c} \simeq \beta_{\text{Ly}\alpha} h\nu_{\text{Ly}\alpha} \frac{Q_{\text{eff}}}{c} \simeq 10^{29} \text{ g cm s}^{-2} \left(\frac{M_*}{100 M_{\odot}}\right), \quad (17)$$

where $L_{\text{Ly}\alpha}$ is the Ly α luminosity due to recombinations in the H II region, in which $\beta_{\text{Ly}\alpha} (\simeq 0.9)$ Ly α photons, each with an energy $h\nu_{\text{Ly}\alpha} = 1.6 \times 10^{-11} \text{ erg}$, are emitted for every recombination (Osterbrock & Ferland 2006; Raiter et al. 2010).⁵ Here, we have also related the number of ionizing photons emitted per second Q to the stellar

mass M_* with equation 13. The momentum of the accretion flow is

$$\dot{M}_{\text{acc}} v \simeq 6 \times 10^{33} \text{ g cm s}^{-2} \left(\frac{v}{10^3 \text{ km s}^{-1}} \right) \left(\frac{\dot{M}_{\text{acc}}}{M_{\odot} \text{ yr}^{-1}} \right), \quad (18)$$

where we have normalized the infall velocity v to its typical value at the edge of the H II region in the solutions shown in Fig. 2, since this is where Lyman α photons will be most strongly coupled to the gas (indeed, these photons are trapped within the accretion flow at r_{HII} , as shown below). Equating these two expressions and using the relation between \dot{M}_{acc} and $M_{*,\text{max}}$ in equation 15, we find the conditions under which Lyman α radiation pressure could halt accretion:

$$v \lesssim 600 \text{ km s}^{-1} \left(\frac{\dot{M}_{\text{acc}}}{0.1 M_{\odot} \text{ yr}^{-1}} \right)^{\frac{1}{7}}. \quad (19)$$

Since the inflow velocity near the edge of the H II region is well above this value at the typical minimum accretion rates we find ($\lesssim 0.1 M_{\odot} \text{ yr}^{-1}$; see Fig. 2), it is clear that Lyman α radiation pressure has only a small impact on accretion in comparison to photoionization pressure. In particular, over the range of stellar masses and critical accretion rates that we consider (Figs. 2 and 3), we find that the infall velocity is \sim three times that in equation 19. In other words, at the high accretion rates we find, the momentum of inflow is always roughly three times what could be countered by Ly α scattering.

It might be thought that if a Lyman α photon is scattered and then traverses the H II region, it could subsequently be scattered many times, thereby enhancing the momentum it imparts the gas (see Adams 1972; Milosavljević et al. 2009). However, upon scattering from an atom in the rapid ($\simeq 10^3 \text{ km s}^{-1}$) accretion flow, the photon would be strongly blue-shifted relative to the gas entering the opposite side of the H II region; as a result, it would couple to gas much less strongly thereafter, greatly limiting the degree to which it could add more momentum to the gas (see Dijkstra & Wyithe 2010, on how galactic outflows enhance Ly α escape by this process).

Furthermore, another effect which dramatically lessens the impact of Ly α photons on accretion is that their large resonant scattering cross section ensures that they are trapped in the H II region and do not scatter out to larger radii. To see this, we follow the formula given by Begelman (1978) for the trapping radius due to Thomson scattering, $r_{\text{trap}} \equiv \dot{M}_{\text{acc}} \sigma_{\text{T}} / 4\pi m_{\text{H}} c$. We define the trapping radius for Ly α photons $r_{\text{Ly}\alpha}$ by substituting the cross section for Lyman α scattering $\sigma_{\text{Ly}\alpha}$ for the Thomson cross section σ_{T} for electron scattering, and by accounting for the fraction of neutral hydrogen atoms off of which Ly α photons can scatter. This yields

$$r_{\text{Ly}\alpha} \simeq 5 \times 10^{24} \text{ cm} \left(\frac{\dot{M}_{\text{acc}}}{M_{\odot} \text{ yr}^{-1}} \right) f_{\text{HI}} \left(\frac{T}{10^4 \text{ K}} \right)^{-\frac{1}{2}}, \quad (20)$$

where f_{HI} is the neutral hydrogen fraction, T is the temperature of the ionized gas, and we have used $\sigma_{\text{Ly}\alpha} = 5.9$

$\times 10^{-14} \text{ cm}^2 (T/10^4 \text{ K})^{-\frac{1}{2}}$ (e.g. Milosavljević et al. 2009). The fraction of neutral hydrogen in the H II region can be estimated by assuming photoionization equilibrium⁶; we obtain

$$f_{\text{HI}} \simeq \frac{4\pi\alpha_{\text{B}} n(r) r^2}{Q_{\text{eff}} \sigma_{\text{HI}}} \\ = 3 \times 10^{-5} \left(\frac{n}{10^{10} \text{ cm}^{-3}} \right) \left(\frac{r}{10^{15} \text{ cm}} \right)^2 \left(\frac{Q_{\text{eff}}}{10^{50} \text{ s}^{-1}} \right)^{-1} \quad (21)$$

where $\sigma_{\text{HI}} = 6 \times 10^{-18} \text{ cm}^2$ is the photoionization cross section for H I (although it is likely slightly lower due to the relatively hard spectrum of the star; see e.g. Johnson & Khochfar 2011). Then with this f_{HI} , Q from equation 13, $n(r)$ from equation 1, and \dot{M}_{acc} in terms of M_* from equation 15, we find:

$$r_{\text{Ly}\alpha} \simeq 10^{12} \text{ cm} \left(\frac{M_*}{100 M_{\odot}} \right)^{\frac{3}{4}} \\ \times \left(\frac{v}{10^3 \text{ km s}^{-1}} \right)^{-1} \left(\frac{T}{10^4 \text{ K}} \right)^{-\frac{1}{2}}. \quad (22)$$

Assuming a temperature of $4 \times 10^4 \text{ K}$ for the photoionized primordial gas (Whalen et al. 2004; Kitayama et al. 2004), Ly α trapping radii for three cases are shown in Fig. 2. We see that $r_{\text{Ly}\alpha}$ is $\sim 2 - 6 r_*$ and is smaller than r_{HII} by roughly an order of magnitude. While this is a modest fraction of the volume of the H II region, because of its steep density profile ($n \propto r^{-2}$) most of the Ly α photons originate from this region.

Integration of equation 3 shows that the fraction of recombinations produced in the H II region as a function of r is $\sim (r_*^{-1} - r^{-1}) / (r_*^{-1} - r_{\text{HII}}^{-1})$. Consequently, the fraction of Ly α photons originating from within the trapping radius is $(r_*^{-1} - r_{\text{Ly}\alpha}^{-1}) / (r_*^{-1} - r_{\text{HII}}^{-1})$, or $\gtrsim 0.5$. Thus, most of them are trapped deep in the H II region and cannot propagate outward to slow accretion at greater radii. Ly α scattering thus removes only $\sim 15\%$ of the momentum of infall, not 30%, so we are justified in neglecting its impact on accretion flow.

At this point, we can show that Ly α photons created outside $r_{\text{Ly}\alpha}$ but within r_{HII} are also trapped in the accretion flow at the boundary of the H II region due to the huge optical depth of the neutral gas to these photons. This is easily shown by equation 20, which for a largely neutral medium (i.e. $f_{\text{HI}} \simeq 1$) yields a trapping radius on the order of 10^{21} cm for the lowest accretion rates given by our solution (equation 12); as this is much larger than both r_{HII} and the Bondi radius, the maximum distance from which the protogalactic gas in can accrete onto the star.⁷ Therefore, we can also safely conclude that Ly α photons will not escape from the H II region to affect the dynamics of the accretion flow at larger radii.

We note that although most Ly α emission is trapped deep in the H II region, the thermal state of the gas may not be greatly affected because cooling via other atomic transitions in hydrogen still occurs (see e.g. Omukai 2001; Raiter et al. 2010; Schleicher et al. 2010). At the high densities within the H II region atoms of both hydrogen and

⁶ Comparing the rates of hydrogen photoionization and collisional ionization using the rate given by Cen (1992), we find that the former is much greater than the latter; thus, photoionization equilibrium is a valid assumption.

⁷ The Bondi radius is roughly $r_{\text{Bondi}} \simeq 10^{16} (M_*/100 M_{\odot}) \text{ cm}$, assuming a sound speed in the protogalactic gas of 10 km s^{-1} , following Wise et al. (2008) and Shang et al. (2010).

helium are readily excited to higher energy ($n > 1$) states by both collisions and absorption of photons; in turn, Lyman series photons (principally Ly α) are easily destroyed by ionizing these excited atoms (see e.g. Osterbrock & Ferland 2006). However, the radiative decay of excited hydrogen atoms also results in significant emission of Balmer series photons as well as two-photon emission from the H(2s) state, to which the H II is much less optically thick. The net result is that the energy in Lyman series photons is reprocessed largely into Balmer series and two-photon continuum emission that escapes the H II region and cools the gas (see e.g. Schleicher et al. 2010). Thus, photoionization heating of the gas can still be balanced by efficient radiative cooling, and even though much of the stellar radiation is reprocessed in the H II region it still eventually emerges and may be observable (see § 4).⁸ It follows that the luminosity of the outgoing radiation is always the same as that of the star; since the star is taken to shine at the Eddington limit, this in turn implies that the force due to electron scattering indeed balances the force due to gravity everywhere in the highly ionized H II region, as we assumed in our calculation. This also suggests that the temperature of the gas is low enough to keep the flow supersonic so gas pressure cannot stop accretion, as we discuss in the Appendix.

Overall, we conclude that it is the momentum imparted to the accreting gas by ionizing photons, despite their being mostly converted to Ly α photons that are in turn converted largely to Balmer series photons, that primarily regulates the growth of supermassive primordial stars.

3. TIME-LIMITED ACCRETION

As noted by Begelman (2010), the lifetime of a very massive primordial star burning nuclear fuel at the Eddington rate L_{Edd} and growing by accretion at a constant rate is $t_{\text{life}} \simeq 4 \text{ Myr}$, twice the lifetime of non-accreting Pop III stars of similar mass.⁹ However, the stellar lifetime is in fact shorter than this for two reasons. First, nuclear fuel must be burned at a higher rate than the Eddington luminosity L_{Edd} in order to support the star against its constantly increasing mass. Thus, the star consumes fuel at the rate given by the sum of the Eddington rate and the rate at which the binding energy of the star increases (Begelman 2010):

$$L_{\text{nuc}} \simeq L_{\text{Edd}} + \frac{GM_* \dot{M}_{\text{acc}}}{r_*} = L_{\text{Edd}} \left(1 + \frac{r_{\text{trap}}}{r_*} \right), \quad (23)$$

where r_* is the radius of the star (equation 14), $r_{\text{trap}} \equiv \dot{M}_{\text{acc}} \sigma_{\text{T}} / 4\pi m_{\text{H}} c = 6 \times 10^{13} \text{ cm}$ ($\dot{M}_{\text{acc}} / \text{M}_{\odot} \text{ yr}^{-1}$) is the radius at which radiation is trapped in the accretion flow by electron scattering, and $L_{\text{Edd}} \equiv 4\pi GM_* m_{\text{H}} c / \sigma_{\text{T}} = 1.2 \times 10^{40} \text{ erg s}^{-1}$ ($M_*/100 \text{ M}_{\odot}$) is the Eddington luminosity for a star of mass M_* . This effect of super-Eddington nuclear

burning contributes to the gradual turnover of the stellar lifetime-limited maximum stellar mass curve shown in red in Figure 3.

While equation (23) is valid when radiation can escape from the stellar surface at r_* and the star is thus thermally relaxed, it ceases to be when radiation is trapped in the accretion flow within a radius r_{trap} above the star due to Thomson scattering. This occurs for accretion rates above $\dot{M}_{\text{acc,trap}} \simeq 4.3 \times 10^{-3} \text{ M}_{\odot} \text{ yr}^{-1} (M_*/100 \text{ M}_{\odot})^{\frac{1}{2}}$. As radiation is trapped in the accretion flow, the accreting material can not radiate its energy within r_{trap} . Upon reaching the stellar surface it therefore deposits energy at a rate $GM_* \dot{M}_{\text{acc}} / r_{\text{trap}}$, instead of at the higher rate $GM_* \dot{M}_{\text{acc}} / r_*$ assumed in equation (23). Therefore, with this substitution is equation (23), at accretion rates $\dot{M}_{\text{acc}} > \dot{M}_{\text{acc,trap}}$ the star consumes fuel as twice the Eddington rate. This results in a decreased lifetime t_{life} , which in turn leads to the sharp turnover of the time-limited maximum stellar mass curve in Figure 3.

The second reason that the stellar lifetime is shortened is also related to the trapping of radiation above the surface of the star, as when this occurs the stellar envelope ceases to be convective (Begelman 2010).¹⁰ This results in the envelope material never reaching the core and being available for fusion. The fuel supply of the star is thus limited to the mass within its convective core, whose fraction of the total mass is (equation 26 of Begelman 2010)

$$\frac{M_{\text{conv}}}{M_*} \simeq 0.54 \left(\frac{r_{\text{trap}}}{r_*} \right)^{\frac{2}{3}} \left(\frac{\dot{M}_{\text{acc}}}{\text{M}_{\odot} \text{ yr}^{-1}} \right)^{-\frac{2}{3}} \left(\frac{M_*}{10^6 \text{ M}_{\odot}} \right)^{\frac{1}{3}}, \quad (24)$$

where we have assumed a central temperature of 10^8 K . This second effect comes into play on the right hand side of the dashed line separating the fully convective regime from the partially convective regime (also separating the regimes in which $r_* > r_{\text{trap}}$ and $r_* < r_{\text{trap}}$).

As shown in Figure 3, these two effects ultimately limit the final mass of the star to $\sim 10^6 \text{ M}_{\odot}$ at the highest accretion rates ($\sim 1 \text{ M}_{\odot} \text{ yr}^{-1}$) found in cosmological simulations of the formation of supermassive stars via direct protogalactic collapse (e.g. Wise et al. 2008; Shang et al. 2010; Johnson et al. 2011). That said, we emphasize that our calculations have been done with significant simplifying assumptions, some of which we briefly discuss in Section 5. In particular, we have adopted a simple model for the evolution of rapidly accreting supermassive stars; however, to be fully confident in our results will require dedicated stellar evolution calculations that account for the continued growth of the star over a large portion of its lifetime (Heger et al. in prep).

Finally, we note that 'dark stars', which are powered by dark matter annihilation, could grow to considerably higher masses than those powered by fusion (e.g. Freese et al. 2008). This is because the cooler surface tem-

⁸ To be precise, for a star with an effective temperature of 10^5 K , roughly 60 percent of its luminosity is emitted in ionizing photons, which are later reprocessed into nebular continuum and recombination emission, such as Ly α .

⁹ This statement assumes that nuclear burning commences when the star has a mass much lower than its final mass. However, we note that for Pop III stars with final masses of $\sim 100 \text{ M}_{\odot}$ nuclear burning may not begin until the star acquires a substantial fraction of its final mass (Omukai & Palla 2003); if so, the lifetime of the star will be much closer to the $\sim 2 \text{ Myr}$ expected for $\gtrsim 100 \text{ M}_{\odot}$ Pop III stars of constant mass.

¹⁰ In this event, the stellar photosphere also expands to r_{trap} , as previous authors have found in the case of accreting primordial protostars (Stahler et al. 1986; Omukai & Palla 2003). Since the internal temperatures of primordial protostars are lower than on the main sequence, their opacities are somewhat higher than those due to Thomson scattering alone. Consequently, their radii are found to swell to more than r_{trap} and perhaps terminate accretion, as discussed in Omukai & Palla (2003).

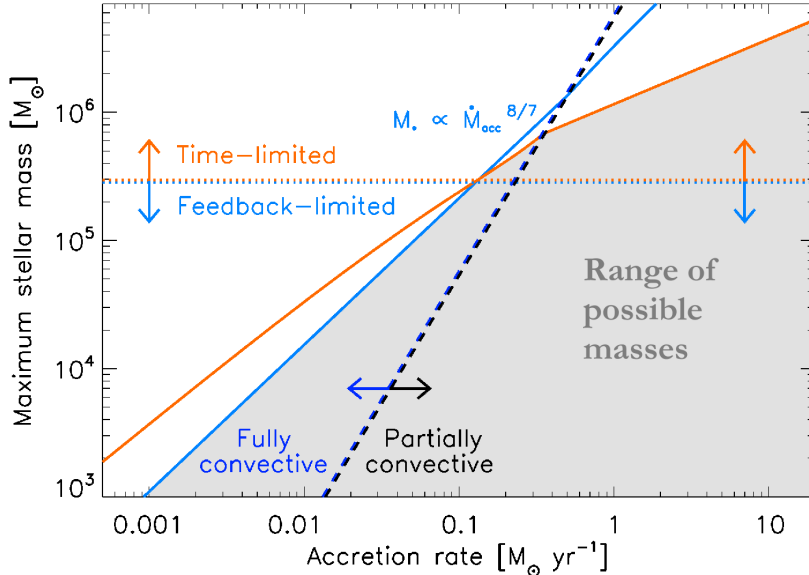


FIG. 3.— The maximum mass to which a star can grow at a constant accretion rate \dot{M}_{acc} . Above the maximum mass $M_* \propto \dot{M}_{\text{acc}}^{8/7}$ given by equation 15 (blue line), radiative feedback shuts off accretion because the H II region of the star breaks out and prevents gas infall. For accretion rates $\gtrsim 10^{-1} M_{\odot} \text{ yr}^{-1}$, the maximum mass is set instead by the lifetime of the star (red line). While at relatively low accretion rates the lifetime of an accreting massive primordial star is ~ 4 Myr, at high accretion rates the stellar lifetime can be shortened dramatically due to the super-Eddington luminosity at which nuclear fuel must be burned to support it during its growth. Also, at high accretion rates (right of the dashed curve), the star ceases to be fully convective and only the material in the convective core of the star is available for nuclear burning, further limiting the lifetime of the supermassive star. The dotted horizontal line marks the mass ($\sim 3 \times 10^5 M_{\odot}$) above which the final mass of a star is dictated by the limited time available for growth and below which it is governed by radiative feedback. The shaded area denotes the range of possible stellar masses for accretion at a constant rate.

peratures of such stars exert much less radiative feedback on accretion and dark matter fuel may last for a much longer time than nuclear fuel. However, recent high resolution cosmological simulations show that primordial stars forming at the centers of dark matter halos may not remain there because of dynamical interactions, as required for the continual capture and annihilation of dark matter in their interiors (Stacy et al. 2011b; Greif et al. 2011). Therefore, it may be that the final masses of dark stars are not so different from those expected for standard primordial stars (see also Ripamonti et al. 2010). If, however, dark stars do grow to be more massive they would exhibit spectral properties distinct from those of solely fusion-powered supermassive Pop III stars (Zackrisson et al. 2010; Ilie et al. 2011), as we discuss next.

4. OBSERVATIONAL SIGNATURES

As supermassive stars are intense sources of radiation that could be detected by current and future surveys, we now examine their observable signatures. The fact that radiative feedback in most cases cannot terminate accretion onto supermassive Pop III stars in collapsing protogalaxies implies that their H II regions will be confined deep in their host halos for most of their lives. It follows that their ionizing radiation is largely reprocessed into nebular emission instead of escaping the halo and reionizing the IGM. As discussed in § 2.2, because the accretion flow is optically thick to the Ly α photons, they cannot directly exit the halo and be observed. These photons are instead further reprocessed largely into Balmer series photons which do escape the H II region and halo and propagate into the

IGM. Therefore, one likely signature of rapidly accreting, isolated supermassive Pop III stars in high-redshift protogalaxies is a strong Balmer line flux accompanied by a conspicuous lack of Ly α emission. A detailed radiative transfer calculation is necessary to quantitatively predict luminosities for all the Balmer lines in hydrogen, but we can place lower limits on the H α flux, which is expected to be the dominant line.

Following Schaerer (2002) and Raiter et al. (2010), we compute the luminosity $L_{\text{H}\alpha}$ in H α as a function of Q_{eff} as discussed in § 2.1. Relating this ionizing photon emission rate to stellar mass with equation 13 yields $L_{\text{H}\alpha} \simeq 4 \times 10^{38} (M_*/100 M_{\odot}) \text{ erg s}^{-1}$; we again emphasize that this is a lower limit because we exclude reprocessing of Ly α into H α , which may dramatically boost H α luminosities above those estimated here. The H α flux at redshift z is

$$f_{\text{H}\alpha} = \frac{L_{\text{H}\alpha}}{4\pi D_L^2} \sim 10^{-20} \text{ erg s}^{-1} \text{ cm}^{-2} \left(\frac{L_{\text{H}\alpha}}{10^{40} \text{ erg s}^{-1}} \right) \left(\frac{1+z}{10} \right)^{-2} \quad (25)$$

where $D_L(z)$ is the luminosity distance to redshift z . We plot this flux as a function of stellar mass and redshift in Figure 4, with the arrows on the H α curves signifying lower limits.

The hard spectrum of ionizing radiation from hot primordial stars also creates an He III region from which a large luminosity in He II $\lambda 1640$ emission is expected (Oh et al. 2001; Tumlinson et al. 2001; Bromm et al. 2001; Schaerer 2002; Johnson et al. 2009). Since the optical depth to this line is low, we also estimate how much of

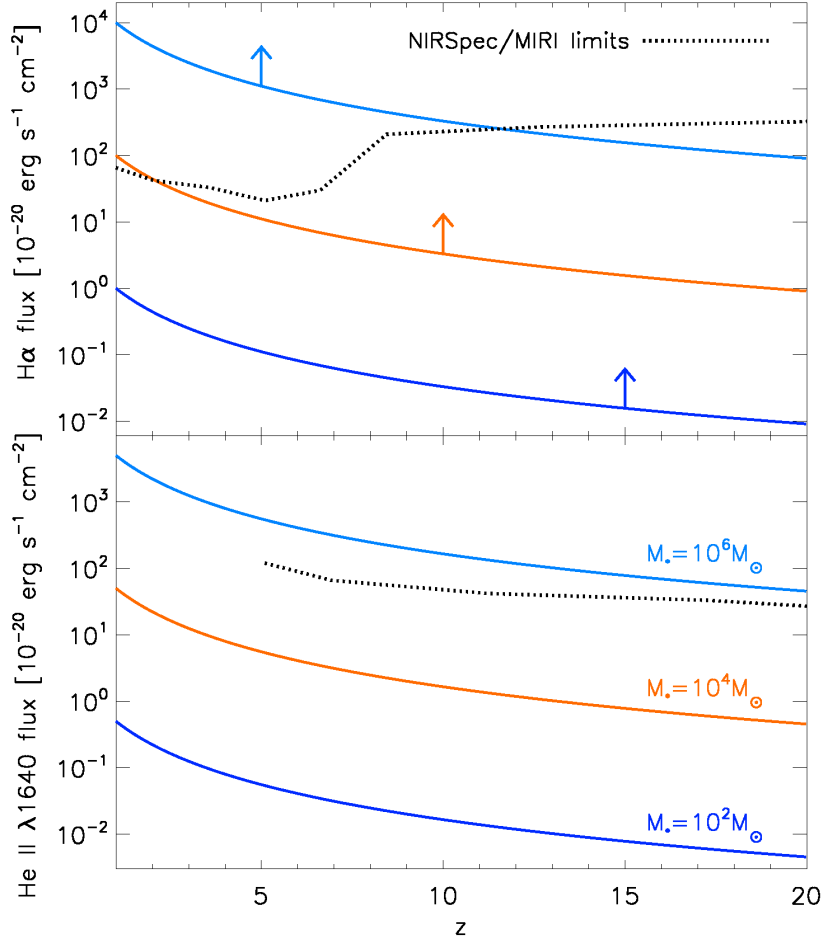


FIG. 4.— The flux in $H\alpha$ (top panel) and $He\ II\ \lambda 1640$ (bottom panel) from accreting main sequence primordial stars, as a function of redshift z , for stellar masses of 10^2 (dark blue), 10^4 (red), and $10^6\ M_{\odot}$ (light blue). The dotted black lines show flux limits for 3σ detection of these lines in 10^4 second exposures with the NIRSpect and MIRI instruments on the *JWST*, operating at resolutions $R = 1000$ and $R = 1200$ - 2400 , respectively. NIRSpect operates at wavelengths of $\simeq 1$ to $5\ \mu\text{m}$, while MIRI covers the range from $\simeq 5$ to $28\ \mu\text{m}$. As discussed in § 4, as we have not accounted for the reprocessing of trapped $Ly\alpha$ photons into Balmer series photons (including $H\alpha$), the $H\alpha$ fluxes shown here are lower limits, as indicated by the arrows. While detection of $H\alpha$ from stars with masses of $\gtrsim 10^4\ M_{\odot}$ may be possible out to very high redshift (e.g. $z \gtrsim 10$), only accreting primordial stars with masses of at least $10^5\ M_{\odot}$ are likely to be detectable in $He\ II\ \lambda 1640$.

its flux exits the halo. For the large ionization rates and densities in our study, we can apply the standard model of Raiter et al. (2010) to compute the luminosity of this line, which we find to be $L_{1640} \simeq 2 \times 10^{38} (M_*/100\ M_{\odot})\ \text{erg s}^{-1}$, where we again have used Table 1 of Bromm et al. (2001) for the number of $He\ II$ -ionizing photons produced as a function of stellar mass. Then, replacing $L_{H\alpha}$ with L_{1640} in equation 34, we derive the flux in the $He\ II\ \lambda 1640$ line, which we plot with $f_{H\alpha}$ in Figure 4 as a function of stellar mass and redshift.

Also shown in Figure 4 are detection limits for two instruments that will be on board the *James Webb Space Telescope* (*JWST*): the Near-Infrared Spectrograph (NIRSpect) and the Mid Infrared Instrument (MIRI). The black dotted curves in Figure 4 denote the flux limits for 3σ detection of the $H\alpha$ and $He\ II\ \lambda 1640$ lines in an exposure time of 10^4 s at resolutions $R = 1000$ for NIRSpect and $R = 1200$ - 2400 for MIRI (Gardner et al. 2006).¹¹ Because ionizing photon rates vary linearly with stellar mass, so

do recombination line fluxes. Consequently, only the more massive accreting primordial stars will be detectable by the *JWST*. Noting again that our $H\alpha$ line fluxes are lower limits, stars with masses $\gtrsim 10^5\ M_{\odot}$ may be detectable in $H\alpha$ out to $z \gtrsim 10$, while accreting stars with masses on the order of $10^4\ M_{\odot}$ could perhaps be detected out to somewhat lower redshift. Detection of the $He\ II\ \lambda 1640$ line will only be possible from stars with masses of at least $10^5\ M_{\odot}$ for sufficiently long exposure times.

We note that the enhanced Balmer line emission from these objects may pose some difficulty to their identification as supermassive Pop III stars. As mentioned earlier, the large ratio of $He\ II\ \lambda 1640$ flux to hydrogen recombination line flux in $Ly\alpha$ or $H\alpha$ is unique to Pop III stars. If, however, much of the $Ly\alpha$ emission is converted to $H\alpha$, the drop in this ratio could mask the primordial nature of the star. That said, the absence of any $Ly\alpha$ emission would still likely reveal the central object to be an accreting supermassive star. Another attribute of rapidly accreting su-

¹¹ *JWST* bandpass data can be found at www.stsci.edu/jwst/science/sensitivity.

permissive stars is strong continuum emission below the Lyman limit, which is the sum of the stellar continuum and the nebular continuum (e.g. Raiter et al. 2010); the latter would be substantial due to the exceptionally high densities expected in the H II regions of these stars. Indeed, it is possible that the sum of the stellar and nebular emission could be detected, for example, in the Deep-Wide Survey to be carried out with the Near-Infrared Camera (NIRCam) on the JWST.

An important obstacle to finding these objects is that their numbers could be small. As discussed by previous authors (Bromm & Loeb 2003; Dijkstra et al. 2004, 2008, see also Agarwal et al. in prep), supermassive stars cannot be so abundant that the black holes they create exceed observed limits on the black hole mass density and x-ray background. This suggests that finding the black holes may be easier than detecting their progenitors. First, they could accrete material for at least 10^8 yr and be luminous for far longer than the stars that created them. Second, future x-ray missions such as the *Joint Astrophysics Nascent Universe Satellite* (JANUS) (Roming 2008; Burrows et al. 2010), *LOBSTER* (Gorenstein 2011), *SVOM* (Götz et al. 2009), and the *Energetic X-ray Imaging Survey Telescope* (EXIST) (Grindlay 2005) will perform all sky surveys with far greater coverage than the JWST. However, if the nascent black hole does not have an accretion disk it may only emit weakly in x-rays at birth (Fryer et al. 2001; Fryer & Heger 2011; Suwa & Ioka 2011, but see also Komissarov & Barkov 2010). If so, the SMBH seed does not become visible until it begins to accrete surrounding protogalactic gas (Haehnelt & Rees 1993; Kuhlen & Madau 2005; Li et al. 2007; Volonteri & Begelman 2010; Johnson et al. 2011).

Supermassive stars could also be detected if they explode as luminous supernovae. However, previous studies have concluded that $\gtrsim 10^3 M_\odot$ Pop III stars collapse to black holes without an explosion (Fuller et al. 1986; Fryer & Heger 2011; Montero et al. 2011) (but see Ohkubo et al. 2006). At 140 - 260 M_\odot , however, pair-instability supernovae occur (Heger et al. 2003) and may be observable by future missions such as the *JWST* (Wise & Abel 2005; Scannapieco et al. 2005; Weinmann & Lilly 2005; Joggerst & Whalen 2011; Kasen et al. 2011). Finally, we note that much of the continuum and line emission from rapidly accreting supermassive stars will appear in the near infrared background (NIRB) today. Although their contribution to the NIRB may be small if they are rare, it could be detected by missions such as the *Cosmic Infrared Background Experiment* (CIBER; e.g. Bock et al. 2006), which is designed to find signatures of primordial galaxy formation at $z \gtrsim 10$.

5. DISCUSSION AND CONCLUSIONS

We find that the masses of the stellar seeds of SMBH forming from baryon collapse in early protogalaxies are primarily governed by their intense ionizing UV flux and their finite lifetimes. For spherically-symmetric accretion at constant rates $\dot{M}_{\text{acc}} \lesssim 0.1 M_\odot \text{ yr}^{-1}$, the maximum mass the star can reach is governed by radiative feedback and is $M_* \simeq 10^3 (\dot{M}_{\text{acc}}/10^{-3} M_\odot \text{ yr}^{-1})^{\frac{5}{7}} M_\odot$. At higher masses, the H II region breaks out to large radii and terminates accretion. We have verified that other forms of feedback,

such as gas pressure, radiation pressure from trapped line emission, photodissociation of H^- , and scattering of Ly α photons are much less effective at slowing accretion (see § 2.2 and the Appendix).

At accretion rates above $\gtrsim 0.1 M_\odot \text{ yr}^{-1}$ the lifetime of the star, not radiative feedback, determines its final mass by limiting the time for which gas can accumulate on the star. Radiative feedback limits supermassive Pop III stars to final masses of $\sim 3 \times 10^5 M_\odot$ and time-limited accretion limits them to $\sim 10^6 M_\odot$ at the highest accretion rates ($\sim 1 M_\odot \text{ yr}^{-1}$) found in numerical simulations of protogalactic collapse (Wise et al. 2008; Shang et al. 2010; Johnson et al. 2011).

We caution that our analytical calculations do not account for all conceivable effects that could stem the growth of supermassive stars. For instance, McKee & Tan (2008) note that rotation of infalling gas leads to lower circumstellar densities and larger H II regions with greater radiative feedback (see also Hosokawa et al. 2011; Stacy et al. 2011a), implying lower final stellar masses. Our spherically-symmetric calculation excludes rotation, so the mass limits we find for a given accretion rate (Fig. 3) are upper limits. We do, however, find agreement with (Omukai & Inutsuka 2002), who performed a similar calculation, although they only considered the growth of stars up to $\sim 10^3 M_\odot$. Furthermore, we also note that the spherical symmetry and constant accretion in our models do not address accretion that is episodic or clumpy and self-shielded from ionizing radiation from the star (Whalen et al. 2008, 2010; Krumholz et al. 2009). These processes could cause accretion to proceed at lower time-averaged rates than those predicted here (but see Kuiper et al. 2011).

Another process that could truncate the growth of supermassive stars well before feedback or stellar lifetimes is the onset of a general relativistic instability in the core of the star that causes it to collapse when it becomes sufficiently massive (Chandrasekhar 1964). Such instabilities are predicted to set in once the star has grown to $\sim 10^5 M_\odot$ (Iben 1963; Fowler 1964), but stellar rotation could stabilize it against collapse up to much larger masses (Fowler 1966; Bisnovatyi-Kogan 1998; Baumgarte & Shapiro 1999). While our models ignore rotation, the accreting gas is likely to have some (e.g. Colgate et al. 2003); if so, the supermassive star will inherit the angular momentum of the gas from which it formed and perhaps bypass the general relativistic instability. Additional insight into the processes that limit the growth of supermassive stars will be gleaned from stellar evolution calculations accounting for the continual accretion of mass at high rates (Heger et al. in prep).

If supermassive stars formed and grew to masses of $\gtrsim 10^5 M_\odot$ in the early universe, recombination emission from their H II regions may be bright enough to be detected by future missions such as the *JWST*. In particular, Ly α photons trapped in the accretion flow are reprocessed into Balmer series photons that could escape into the IGM. Consequently, the formation of these objects is accompanied by distinctive strong H α emission together with strong continuum and He II $\lambda 1640$ emission, the latter arising from the hard spectrum of hot Pop III stars. However, their black holes may be easier to discover in observational

surveys, given the small numbers and brief lifetimes of their progenitors. Indeed, these black holes may be the very ones that have already been found at the centers of massive galaxies and quasars at high redshifts.

Current numerical simulations of SMBH seed formation in early protogalaxies are now at an impasse because the formation of the hydrostatic supermassive protostar restricts Courant times to values that are too short to evolve central flows for even one dynamical time (but see Johnson et al. 2011 for an alternative approach using the sink particle technique). Our results suggest that in the early and intermediate stages of the growth of the star its evolution is essentially decoupled from flows on even slightly larger spatial scales. Consequently, it should now be possible to retreat from the extreme spatial resolutions previously applied to the protostar and evolve flows at the center of the galaxy over enough dynamical times to capture its structure at the time of the death of the star and breakout of x-rays from the BH seed into the IGM. Thus, it will soon

be possible to witness the births of the first quasars in the universe with supercomputers.

ACKNOWLEDGEMENTS

We gratefully acknowledge the support of the U.S. Department of Energy through the LANL/LDRD Program for this work. We would like to thank Stirling Colgate, Dave Collins, Alex Heger, Kevin Honnell, Sadegh Khochfar, Tsing-Wai Wong, and Hao Xu for helpful discussions. This work also benefited from the constructive comments of an anonymous reviewer. JLJ gratefully acknowledges the support of a LANL LDRD Director's Postdoctoral Fellowship at Los Alamos National Laboratory. DJW acknowledges support from the Bruce and Astrid McWilliams Center for Cosmology at CMU. Work at LANL was done under the auspices of the National Nuclear Security Administration of the U.S. Department of Energy at Los Alamos National Laboratory under Contract No. DE-AC52-06NA25396.

REFERENCES

- Abel, T., Anninos, P., Zhang, Y., & Norman, M. L. 1997, *New A*, 2, 181
- Abel, T., Bryan, G. L., & Norman, M. L. 2002, *Science*, 295, 93
- Adams, T. F. 1972, *ApJ*, 174, 439
- Alexander, D. M. & Hickox, R. C. 2011, ArXiv e-prints
- Alvarez, M. A., Bromm, V., & Shapiro, P. R. 2006, *ApJ*, 639, 621
- Alvarez, M. A., Wise, J. H., & Abel, T. 2009, *ApJ*, 701, L133
- Baumgarte, T. W. & Shapiro, S. L. 1999, *ApJ*, 526, 941
- Begelman, M. C. 1978, *MNRAS*, 184, 53
- . 2010, *MNRAS*, 402, 673
- Begelman, M. C., Volonteri, M., & Rees, M. J. 2006, *MNRAS*, 370, 289
- Bisnovaty-Kogan, G. S. 1998, *ApJ*, 497, 559
- Bock, J., Battle, J., Cooray, A., Kawada, M., Keating, B., Lange, A., Lee, D.-H., Matsumoto, T., Matsuura, S., Pak, S., Renbarger, T., Sullivan, I., Tsumura, K., Wada, T., & Watabe, T. 2006, *New A Rev.*, 50, 215
- Braun, E. & Dekel, A. 1989, *ApJ*, 345, 31
- Bromm, V., Coppi, P. S., & Larson, R. B. 2002, *ApJ*, 564, 23
- Bromm, V., Kudritzki, R. P., & Loeb, A. 2001, *ApJ*, 552, 464
- Bromm, V. & Loeb, A. 2003, *ApJ*, 596, 34
- Burrows, D. N., Roming, P. W. A., Fox, D. B., Herter, T. L., Falcone, A., Bilén, S., Nousek, J. A., & Kennea, J. A. 2010, in Presented at the Society of Photo-Optical Instrumentation Engineers (SPIE) Conference, Vol. 7732, Society of Photo-Optical Instrumentation Engineers (SPIE) Conference Series
- Carr, B. J., Kohri, K., Sendouda, Y., & Yokoyama, J. 2010, *Phys. Rev. D*, 81, 104019
- Cen, R. 1992, *ApJS*, 78, 341
- Chandrasekhar, S. 1964, *ApJ*, 140, 417
- Chuzhoy, L., Kuhlen, M., & Shapiro, P. R. 2007, *ApJ*, 665, L85
- Clark, P. C., Glover, S. C. O., Smith, R. J., Greif, T. H., Klessen, R. S., & Bromm, V. 2011, *Science*, 331, 1040
- Colgate, S. A., Cen, R., Li, H., Currier, N., & Warren, M. S. 2003, *ApJ*, 598, L7
- Devecchi, B. & Volonteri, M. 2009, *ApJ*, 694, 302
- Dijkstra, M., Haiman, Z., & Loeb, A. 2004, *ApJ*, 613, 646
- Dijkstra, M., Haiman, Z., Mesinger, A., & Wyithe, J. S. B. 2008, *MNRAS*, 391, 1961
- Dijkstra, M. & Wyithe, J. S. B. 2010, *MNRAS*, 408, 352
- Djorgovski, S. G., Volonteri, M., Springel, V., Bromm, V., & Meylan, G. 2008, in The Eleventh Marcel Grossmann Meeting On Recent Developments in Theoretical and Experimental General Relativity, Gravitation and Relativistic Field Theories, ed. H. Kleiner, R. T. Jantzen, & R. Ruffini, 340–367
- Doroshkevich, A. G. & Kolesnik, I. G. 1976, *SvA*, 53, 10
- Dotan, C., Rossi, E. M., & Shaviv, N. J. 2011, *MNRAS*, 417, 3035
- Elitzur, M. & Ferland, G. J. 1986, *ApJ*, 305, 35
- Fan, X., Strauss, M. A., Schneider, D. P., Becker, R. H., White, R. L., Haiman, Z., Gregg, M., Pentericci, L., Grebel, E. K., Narayanan, V. K., Loh, Y., Richards, G. T., Gunn, J. E., Lupton, R. H., Knapp, G. R., Ivezić, Ž., Brandt, W. N., Collinge, M., Hao, L., Harbeck, D., Prada, F., Schaye, J., Strateva, I., Zakamska, N., Anderson, S., Brinkmann, J., Bahcall, N. A., Lamb, D. Q., Okamura, S., Szalay, A., & York, D. G. 2003, *AJ*, 125, 1649
- Fowler, W. A. 1964, *Reviews of Modern Physics*, 36, 545
- . 1966, *ApJ*, 144, 180
- Freese, K., Spolyar, D., & Aguirre, A. 2008, *J. Cosmology Astropart. Phys.*, 11, 14
- Fryer, C. L. & Heger, A. 2011, *Astronomische Nachrichten*, 332, 408
- Fryer, C. L., Woosley, S. E., & Heger, A. 2001, *ApJ*, 550, 372
- Fuller, G. M., Woosley, S. E., & Weaver, T. A. 1986, *ApJ*, 307, 675
- Gorenstein, P. 2011, in Society of Photo-Optical Instrumentation Engineers (SPIE) Conference Series, Vol. 8147, Society of Photo-Optical Instrumentation Engineers (SPIE) Conference Series
- Götz, D., Paul, J., Basa, S., Wei, J., Zhang, S. N., Atteia, J.-L., Barret, D., Cordier, B., Claret, A., Deng, J., Fan, X., Hu, J. Y., Huang, M., Mandrou, P., Mereghetti, S., Qiu, Y., & Wu, B. 2009, in American Institute of Physics Conference Series, Vol. 1133, American Institute of Physics Conference Series, ed. C. Meegan, C. Kouveliotou, & N. Gehrels, 25–30
- Greif, T. H., Springel, V., White, S. D. M., Glover, S. C. O., Clark, P. C., Smith, R. J., Klessen, R. S., & Bromm, V. 2011, *ApJ*, 737, 75
- Grindlay, J. E. 2005, *New A Rev.*, 49, 436
- Haehnel, M. G. & Rees, M. J. 1993, *MNRAS*, 263, 168
- Heger, A., Fryer, C. L., Woosley, S. E., Langer, N., & Hartmann, D. H. 2003, *ApJ*, 591, 288
- Hosokawa, T., Omukai, K., Yoshida, N., & Yorke, H. W. 2011, ArXiv e-prints
- Hummer, D. G. & Storey, P. J. 1987, *MNRAS*, 224, 801
- Iben, Jr., I. 1963, *ApJ*, 138, 1090
- Ilie, C., Freese, K., Valluri, M., Iliev, I. T., & Shapiro, P. 2011, ArXiv e-prints
- Inayoshi, K. & Omukai, K. 2011, *MNRAS*, 416, 2748
- Jeon, M., Pawlik, A. H., Greif, T. H., Glover, S. C. O., Bromm, V., Milosavljevic, M., & Klessen, R. S. 2011, ArXiv e-prints
- Joggerst, C. C. & Whalen, D. J. 2011, *ApJ*, 728, 129
- Johnson, J. L. & Bromm, V. 2007, *MNRAS*, 374, 1557
- Johnson, J. L., Greif, T. H., Bromm, V., Klessen, R. S., & Ippolito, J. 2009, *MNRAS*, 399, 37
- Johnson, J. L. & Khochfar, S. 2011, ArXiv e-prints
- Johnson, J. L., Khochfar, S., Greif, T. H., & Durier, F. 2011, *MNRAS*, 410, 919
- Kasen, D., Woosley, S. E., & Heger, A. 2011, ArXiv e-prints
- Khlopov, M. Y. 2010, *Research in Astronomy and Astrophysics*, 10, 495
- Kitayama, T., Yoshida, N., Susa, H., & Umemura, M. 2004, *ApJ*, 613, 631
- Koushiappas, S. M., Bullock, J. S., & Dekel, A. 2004, *MNRAS*, 354, 292
- Krumholz, M. R., Klein, R. I., McKee, C. F., Offner, S. S. R., & Cunningham, A. J. 2009, *Science*, 323, 754
- Kuhlen, M. & Madau, P. 2005, *MNRAS*, 363, 1069
- Kuiper, R., Klahr, H., Beuther, H., & Henning, T. 2011, ArXiv e-prints
- Li, Y. 2011, ArXiv e-prints
- Li, Y., Hernquist, L., Robertson, B., Cox, T. J., Hopkins, P. F., Springel, V., Gao, L., Di Matteo, T., Zentner, A. R., Jenkins, A., & Yoshida, N. 2007, *ApJ*, 665, 187

- Lodato, G. & Natarajan, P. 2006, MNRAS, 371, 1813
Mack, K. J., Ostriker, J. P., & Ricotti, M. 2007, ApJ, 665, 1277
Madau, P. & Rees, M. J. 2001, ApJ, 551, L27
McKee, C. F. & Tan, J. C. 2008, ApJ, 681, 771
Milosavljević, M., Bromm, V., Couch, S. M., & Oh, S. P. 2009, ApJ, 698, 766
Montero, P. J., Janka, H.-T., & Mueller, E. 2011, ArXiv e-prints
Mortlock, D. J., Warren, S. J., Venemans, B. P., Patel, M., Hewett, P. C., McMahon, R. G., Simpson, C., Theuns, T., González-Solares, E. A., Adamson, A., Dye, S., Hambly, N. C., Hirst, P., Irwin, M. J., Kuiper, E., Lawrence, A., & Röttgering, H. J. A. 2011, Nature, 474, 616
Nakamura, F. & Umemura, M. 2001, ApJ, 548, 19
Oh, S. P. & Haiman, Z. 2002, ApJ, 569, 558
Oh, S. P., Haiman, Z., & Rees, M. J. 2001, ApJ, 553, 73
Ohkubo, T., Nomoto, K., Umeda, H., Yoshida, N., & Tsuruta, S. 2009, ApJ, 706, 1184
Ohkubo, T., Umeda, H., Maeda, K., Nomoto, K., Suzuki, T., Tsuruta, S., & Rees, M. J. 2006, ApJ, 645, 1352
Omukai, K. 2001, ApJ, 546, 635
Omukai, K. & Inutsuka, S.-i. 2002, MNRAS, 332, 59
Omukai, K. & Palla, F. 2001, ApJ, 561, L55
— 2003, ApJ, 589, 677
Omukai, K., Schneider, R., & Haiman, Z. 2008, ApJ, 686, 801
O’Shea, B. W. & Norman, M. L. 2007, ApJ, 654, 66
Osterbrock, D. E. & Ferland, G. J. 2006, Astrophysics of gaseous nebulae and active galactic nuclei, ed. Osterbrock, D. E. & Ferland, G. J.
Park, K. & Ricotti, M. 2011, ApJ, 739, 2
Pelupessy, F. I., Di Matteo, T., & Ciardi, B. 2007, ApJ, 665, 107
Raiter, A., Schaerer, D., & Fosbury, R. A. E. 2010, A&A, 523, A64
Regan, J. A. & Haehnelt, M. G. 2009, MNRAS, 396, 343
Ripamonti, E., Iocco, F., Ferrara, A., Schneider, R., Bressan, A., & Marigo, P. 2010, MNRAS, 406, 2605
Roming, P. 2008, in COSPAR, Plenary Meeting, Vol. 37, 37th COSPAR Scientific Assembly, 2645–+
Scannapieco, E., Madau, P., Woosley, S., Heger, A., & Ferrara, A. 2005, ApJ, 633, 1031
Schaerer, D. 2002, A&A, 382, 28
Schleicher, D. R. G., Spaans, M., & Glover, S. C. O. 2010, ApJ, 712, L69
Sethi, S., Haiman, Z., & Pandey, K. 2010, ApJ, 721, 615
Shang, C., Bryan, G. L., & Haiman, Z. 2010, MNRAS, 402, 1249
Shibata, M. & Shapiro, S. L. 2002, ApJ, 572, L39
Spaans, M. & Silk, J. 2006, ApJ, 652, 902
Spitzer, L. 1978, Physical processes in the interstellar medium, ed. Spitzer, L.
Stacy, A., Greif, T. H., & Bromm, V. 2010, MNRAS, 403, 45
— 2011a, ArXiv e-prints
Stacy, A., Pawlik, A. H., Bromm, V., & Loeb, A. 2011b, ArXiv e-prints
Stahler, S. W., Palla, F., & Salpeter, E. E. 1986, ApJ, 302, 590
Suwa, Y. & Ioka, K. 2011, ApJ, 726, 107
Tanaka, T. & Haiman, Z. 2009, ApJ, 696, 1798
Tumlinson, J., Giroux, M. L., & Shull, J. M. 2001, ApJ, 550, L1
Turk, M. J., Abel, T., & O’Shea, B. 2009, Science, 325, 601
Volonteri, M. 2010, A&A Rev., 18, 279
Volonteri, M. & Begelman, M. C. 2010, MNRAS, 409, 1022
Weinmann, S. M. & Lilly, S. J. 2005, ApJ, 624, 526
Whalen, D., Abel, T., & Norman, M. L. 2004, ApJ, 610, 14
Whalen, D., Hueckstaedt, R. M., & McConkie, T. O. 2010, ApJ, 712, 101
Whalen, D., O’Shea, B. W., Smidt, J., & Norman, M. L. 2008, ApJ, 679, 925
Willott, C. J., McLure, R. J., & Jarvis, M. J. 2003, ApJ, 587, L15
Wise, J. H. & Abel, T. 2005, ApJ, 629, 615
Wise, J. H., Turk, M. J., & Abel, T. 2008, ApJ, 682, 745
Wishart, A. W. 1979, MNRAS, 187, 59P
Wolcott-Green, J., Haiman, Z., & Bryan, G. L. 2011, MNRAS, 418, 838
Wyithe, S. & Loeb, A. 2011, ArXiv e-prints
Yoshida, N., Omukai, K., & Hernquist, L. 2008, Science, 321, 669
Zackrisson, E., Scott, P., Rydberg, C.-E., Iocco, F., Edvardsson, B., Östlin, G., Sivertsson, S., Zitrin, A., Broadhurst, T., & Gondolo, P. 2010, ApJ, 717, 257

APPENDIX

NEGLECTED FEEDBACK PROCESSES

Here, we discuss several processes which have a negligible impact on our estimate of the the final maximum stellar mass given by equation 15.

He II Photoionization

To assess the relative importance of He II photoionization in slowing the accretion flow in the He III region, we follow the argument in Section 2.1 for He I photoionization. For the ratio of He II photoionization pressure to H I photoionization pressure, we have

$$\frac{p_{\text{HeII}}}{p_{\text{HI}}} \simeq \frac{n_{\text{He}}}{n_{\text{H}}} \frac{h\nu_{\text{HeII}}}{h\nu_{\text{HI}}} \frac{\alpha_{\text{B,HeII}}}{\alpha_{\text{B,HI}}} \simeq 1.1, \quad (\text{A1})$$

where we have taken it that $h\nu_{\text{HeII}}/h\nu_{\text{HI}} \simeq 54.4 \text{ eV} / 29 \text{ eV} \simeq 1.8$, and that $\alpha_{\text{B,HeII}}/\alpha_{\text{B,HI}} \simeq 6.4$ (Osterbrock & Ferland 2006). Therefore, within the He III region, the radiation pressures due to He II and H I photoionizations are comparable. This is convenient because in the He III region it is recombination emission from He II, not stellar photons, which largely keeps hydrogen photoionized (Osterbrock & Ferland 2006). Therefore, while this diffuse recombination emission does not transfer appreciable outward momentum to the gas, the stellar photons that ionize He II transfer roughly the same momentum to the gas that they would in ionizing H I. As a consequence, solving in detail for the pressure due to He II photoionization would result in an almost identical solution to the one we have found by just treating the H II region.

H⁻ Photodetachment

In order for very high accretion rates onto a supermassive star in a primordial protogalaxy to be realized, the H₂ fraction in the accreting protogalactic gas must be very low (Bromm & Loeb 2003; Lodato & Natarajan 2006; Spaans & Silk 2006; Omukai et al. 2008; Wise et al. 2008). Indeed, the $\gtrsim 10^4 \text{ K}$ virial temperatures at the centers of $10^7 - 10^8 M_{\odot}$ halos heavily suppress H₂ fractions, so it is a good approximation to take it that the opacity due to absorption of photons by H₂ is also low. However, this does not imply that H⁻ fractions are negligible because it forms from reactants whose abundances are not suppressed by H₂-dissociating backgrounds or high virial temperatures:



where γ denotes the emission of a photon. In principle, the absorption of photons with energies $\geq 0.75 \text{ eV}$ by photodetachment of H⁻ could be an important channel by which momentum can be imparted to inflow. To determine the rate at which momentum that could be transferred to the gas, it suffices to estimate the equilibrium rate of H⁻ formation,

since this is also the rate at which H^- will be destroyed and momentum will be acquired by the gas (see Abel et al. 1997; Chuzhoy et al. 2007). Using the density profiles from our calculations, which assume that the gas falls toward the star at the free-fall velocity above r_{HII} (Fig. 2), we have $n(r) \lesssim 10^{12} (r/r_{\text{HII}})^{-\frac{3}{2}} \text{ cm}^{-3}$. Numerical simulations of protogalactic collapse predict central free electron fractions $f_e \sim 10^{-4}$ (e. g. Shang et al. 2010). With these as upper limits along with the rate coefficient k_{H^-} for H^- formation, integration over the density profile of the halo yields the H^- formation rate Q_{H^-} outside the H II region:

$$Q_{\text{H}^-} \lesssim k_{\text{H}^-} \int_{r_{\text{HII}}}^{r_{\text{outer}}} 4\pi r^2 f_e n^2 dr \simeq 10^{44} \text{ s}^{-1}, \quad (\text{A3})$$

where $k_{\text{H}^-} \sim 10^{-14} \text{ cm}^3 \text{ s}^{-1}$ (Wishart 1979; Abel et al. 1997). We assume that hydrogen is predominantly neutral outside the H II region and neglect the small H^- fractions that may form in the H II region. Finally, to ensure that we have found a strong upper limit, we integrate this profile out to $r_{\text{outer}} = 10^{21} \text{ cm}$, which is approximately the virial radius of the atomically-cooled halos at high redshift that host the supermassive stars we are studying. Even allowing for the high average photon energy for photodetachment $h\nu_{\text{H}^-} \sim 10 \text{ eV}$ for supermassive Pop III stars, the maximum momentum that could be transferred to the gas per unit time is

$$\frac{h\nu_{\text{H}^-} Q_{\text{H}^-}}{c} \lesssim 10^{22} \text{ g cm s}^{-2}. \quad (\text{A4})$$

This is orders of magnitude smaller than the momentum of the accretion flow in equation 18, so H^- destruction does not contribute to radiative feedback.

Radiation Pressure from Trapped Ly α and Balmer Series Lines

In Section 2.2, we raised the possibility that Ly α photons may slow down accretion by scattering from neutral atoms at the edge of the H II region. While we showed that this is unlikely to alter the flow, mostly because Ly α photons are confined to $r_{\text{Ly}\alpha}$, radiation pressure due to nebular emission lines in optically thick gas may be sufficient to reduce accretion. As also mentioned in Section 2.2, trapped Ly α photons may be largely converted to Balmer series photons, in some cases after being destroyed by absorption by excited hydrogen or helium (Osterbrock & Ferland 2006). These Balmer photons can then propagate outward and efficiently cool the gas. The high temperatures, densities, and Ly α photons trapped in the H II region cause a large fraction of the hydrogen atoms to be excited to the $n = 2$ state there. From this state, either collisions or absorptions will further excite the atoms, which often later decay by emitting a Balmer series photon.

To evaluate the degree to which radiation pressure from trapped line photons alters the dynamics of accretion, we first estimate the optical depth to Balmer photons both inside and outside the H II region. Within r_{HII} , the density of neutral hydrogen atoms can be estimated from equation 21 and assuming that $n \propto r^{-2}$, as implied by the nearly constant velocity profile of the gas in the H II region (Fig. 2). The neutral hydrogen column density N_{H} through the H II region is then

$$\begin{aligned} N_{\text{H}}(< r_{\text{HII}}) &\simeq \int_{r_*}^{r_{\text{HII}}} f_{\text{HI}}(r) n(r) dr \\ &= f_{\text{HI}}(r_{\text{HII}}) n(r_{\text{HII}}) \frac{r_{\text{HII}}^2}{r_*} \simeq 10^{17} \text{ cm}^{-2}, \end{aligned} \quad (\text{A5})$$

which, from the scaling in the second equation, can be shown to have only a weak dependence on the stellar mass for $M_* = 10^2 - 10^6 M_{\odot}$ for our solutions to the minimum accretion rate. The cross sections for absorption of Balmer series photons by H in the $n = 2$ state are 19, 3.5, and $1.3 \times 10^{-17} \text{ cm}^2$ for H α , H β , and H γ , respectively. The higher energy Balmer series cross sections are all below these values. With these cross sections and $N_{\text{H}}(< r_{\text{HII}})$, we can express the optical depth through the H II region solely as a function of the relative populations N_2/N_1 of the $n = 1$ and $n = 2$ levels of neutral hydrogen in the H II region. We find that even for N_2/N_1 as high as ~ 0.05 , the H II region is optically thin to all Balmer series photons, while the largest optical depth possible for H α is $\tau_{\text{H}\alpha} \simeq 20$. However, this is still far below the optical depth for Ly α photons, and Balmer series photons will eventually leak out of the H II region, although in some cases only after a number of scatterings. Therefore, while Ly α photons in general will not escape the H II region, Balmer series photons will escape and allow the gas to radiatively cool, as we noted in Section 2.2.

Next, we consider the optical depth to Balmer series lines outside the H II region. In this region, we set $f_{\text{HI}} = 1$ and adopt a free-fall density profile $n \propto r^{-\frac{3}{2}}$ for the gas, as in Section 2.1. The neutral hydrogen column density beyond r_{HII} is then

$$\begin{aligned} N_{\text{H}}(> r_{\text{HII}}) &\simeq \int_{r_{\text{HII}}}^{\infty} n(r) dr \\ &= 2n(r_{\text{HII}})r_{\text{HII}} \simeq 10^{24} \text{ cm}^{-2}, \end{aligned} \quad (\text{A6})$$

which again is not strongly dependent on stellar mass.

Because the gas outside the H II region is well below the critical density at which excited levels in hydrogen would be populated and kept in equilibrium by collisions (and because Ly α photons are mostly trapped in the H II region and cannot excite neutral hydrogen beyond r_{HII}), the relative population of the $n = 2$ level of hydrogen is expected to be very small. In this case, Schleicher et al. (2010) find that in general $N_2/N_1 \lesssim 10^{-10}$. With this as an upper limit and the cross

sections for Balmer series photon absorption above, we find that the optical depths to Balmer series lines are $\tau_{H\alpha} \sim 4 \times 10^{-2}$, $\tau_{H\beta} \sim 8 \times 10^{-3}$, and $\tau_{H\gamma} \sim 3 \times 10^{-3}$. At such low optical depths, Balmer series photons will propagate largely unimpeded through the inflow and, most likely, exit the halo with minimal effect on accretion. As these photons also move freely through the intergalactic medium (IGM), accreting supermassive stars probably have a distinctive observational signature, as we discussed in §4.

Thus, because outside the H II region the optical depth to Balmer series photons is small and Ly α photons cannot propagate across the H II region boundary, we conclude that radiation pressure due to trapped emission lines will not be appreciable beyond r_{HII} . However, it may be that this pressure is substantial within the H II region. To estimate its magnitude, we compare it to the ram pressure of the accretion flow. For the latter, we have

$$P_{\text{ram}} = n\mu m_{\text{H}}v^2 \simeq 50 \left(\frac{\dot{M}_{\text{acc}}}{M_{\odot} \text{ yr}^{-1}} \right) \left(\frac{r}{10^{15} \text{ cm}} \right)^{-2} \left(\frac{v}{100 \text{ km s}^{-1}} \right) \text{ dyn cm}^{-2}, \quad (\text{A7})$$

where we have used equation 1 to express n in terms of v and \dot{M}_{acc} . We use the prescription of Braun & Dekel (1989) for the radiation pressure (see also Elitzur & Ferland 1986):

$$P_{\text{line}} = \left(\frac{4\pi}{9c} \right) \left(\frac{2h\nu_{\text{tran}}^3}{c^2} \right) \frac{N_{i+1}}{N_i} \Delta\nu_{\text{tran}}, \quad (\text{A8})$$

where N_{i+1}/N_i is the ratio of the upper and lower level populations for the given transition, whose frequency is ν_{tran} . The line width $\Delta\nu_{\text{tran}} \sim 2 \times 10^{11} (T/10^4 \text{ K})^{\frac{1}{2}} (\ln \tau)^{\frac{1}{2}} \text{ s}^{-1}$, where τ is the optical depth of the line.

Assuming optical depths $\tau_{\text{Ly}\alpha} = 10^4$ and $\tau_{\text{Balmer}} = 20$, both of which are rough upper limits in the H II region, and $N_{i+1}/N_i = 1$ in both cases, we find strong upper limits of $\sim 6 \text{ dyn cm}^{-2}$ and $2 \times 10^{-2} \text{ dyn cm}^{-2}$ for the Ly α and Balmer line radiation pressures, respectively. Comparing these pressures to P_{ram} at r_{HII} , which is a lower limit for the H II region due to its strong dependence on r in equation A7, we find that it is always at least a factor of ~ 4 larger than radiation pressure from optically thick lines. Therefore, lines will not play a large role in slowing accretion in the H II region.

Gas Pressure

Because infall is highly supersonic, gas pressure cannot decelerate the gas (Omukai & Inutsuka 2002). We have verified that this holds even when a gas pressure term is included in the equation of motion. We find that only for extremely high sound speeds corresponding to temperatures of at least 10^6 K would gas pressure begin to impact the dynamics of the accretion flow. However, temperatures this high are not found in numerical simulations of protogalactic collapse (Wise et al. 2008; Regan & Haehnelt 2009; Shang et al. 2010; Johnson et al. 2011) or in H II regions because the Balmer thermostat limits ionized gas temperatures to at most a few $\times 10^4 \text{ K}$.

Accretion Luminosity

Our conclusions regarding the maximum mass of the supermassive star rest on the assumption that the critical accretion rate for a given stellar mass (equation 12) separates two regimes: below this rate, accretion is suppressed by radiative feedback and above this rate accretion proceeds. As shown in Section 2.1, it is clear that accretion is prevented for inflow rates below the critical rate because the ionization front breaks out to infinity and photoionization pressure halts infall at all radii. For accretion rates above the critical rate, the flow will arrive at the star with a velocity $v(r_*) > 0$. This implies that the accreting material will have some kinetic energy that must be dissipated at the stellar surface, some portion of which will be radiation. This radiation could slow accretion within the H II region by electron scattering or photoionizations.

Let us assume that all of the kinetic energy of the flow is converted to radiation that propagates outward on impact with the star at some velocity $v(r_*)$. The luminosity thus generated is

$$L_{\text{acc}} = \frac{\dot{M}_{\text{acc}}v^2}{2}, \quad (\text{A9})$$

which yields a total momentum in photons of $L_{\text{acc}}/c = \dot{M}_{\text{acc}}v^2/2c$. Comparing this to the momentum of the infalling gas, $\dot{M}_{\text{acc}}v$, we see that the momentum in the accretion luminosity is a factor $v/2c$ lower than that of the gas. Therefore, accretion radiation cannot halt the flow in the steady-state approximation. However, bouts of massive accretion could in principle generate enough radiation to slow infall at larger radii where gas has a lower momentum, like the episodic accretion onto black holes in the early universe discussed by Milosavljević et al. (2009).

We note that an additional effect of accretion at very high rates (much higher than those in equation 12) is the trapping of radiation by electron scattering or other sources of opacity in the flow (e.g. Begelman 1978, 2010; Wyithe & Loeb 2011). As discussed by Omukai & Palla (2003, see also Stahler et al. 1986) in the context of primordial protostellar accretion, radiation trapping can lead to rapid expansion of the stellar photosphere that halts the growth of the star. We note, however, that such expansion also causes the effective temperature of the star to fall with the increase in surface area of the photosphere¹², which in turn leads to a softening of the emitted radiation and a lower ionizing photon emission rate Q . This, and the fact that accretion rates greater than those in equation 12 result in smaller H II regions, suggests that the flow cannot be stopped, at least not by photoionization pressure.

¹² At constant luminosity, the effective temperature at the stellar photosphere scales as $T_{\text{eff}} \propto r_*^{-\frac{1}{2}}$